2022 12th Workshop on Hyperspectral Imaging and Signal Processing: Evolution in Remote Sensing (WHISPERS) | 978-1-6654-7069-8/22/$31.00 ©2022 IEEE | DOI: 10.1109/WHISPERS56178.2022.9955135

ESTIMATION OF THE LOWER HEATING VALUE OF SOLID RECOVERED FUEL BASED ON SWIR HYPER-SPECTRAL IMAGES AND MACHINE LEARNING

S. Verga†, M. Compare†,‡, E. Zio †,‡,#,##, G. Carra, M. Farina*, I. Righetto*, V. Sala***
†Aramis s.r.l., ‡Dido s.r.l., # Politecnico di Milano, ##Mines ParisTech, *a2a S.p.A., **Images S.p.A

ABSTRACT

In this work, we apply Machine Learning techniques to Hyper-Spectral Images acquired by a Short Wave Infra-Red (SWIR) Camera, to classify the materials composing the Solid Recovered Fuel (SRF). This classification, enabled by data pre-processing techniques, is used to estimate the Lower Heat Value (LHV) of SRF samples, building on models of the literature. The accurate and timely estimates of SRF LHVs yield significant benefits to SRF consumers.

Index Terms— Solid Recovered Fuel, Lower Heat Value, SWIR, LR-Classifier

1. INTRODUCTION

Solid Recovered Fuel (SRF) mainly consists of combustible components, including paper, woods, non-recyclable plastics, textiles, etc., which are selected from municipal, industrial and commercial solid waste materials.

Nowadays, SRF is largely used in energy intensive productions, such as cement kilns, waste-to-energy and thermal power plants. This yields huge environmental benefits, as SRF ensures energy for industrial processes and domestic heating, while reducing the global greenhouse gas emission and providing a complementary solution to the waste recycling priority ([1]).

In addition to the fulfillment of the stringent requirements defined by environment international standards, SRF is also expected to meet demanding quality requirements that ensure the efficiency of the waste to energy conversion and the continuity of the production ([2], [3]). For example, to increase the energy production efficiency, we need to reduce the fluctuations in the SRF energy release rate, thus avoiding the abrupt changes that challenge the heating process control [4]. Yet, to both avoid the corrosion of the plant components and produce high quality cement, we must avoid high concentration of chlorine in SRF. From this, it clearly emerges that accurately estimating the main characteristics of the SRF such as the Lower Heat Value (LHV), humidity, quantity of chlorine and mercury, considerably increases the market value of the SRF, as these pieces of information are relevant for the SRF consumers.

With respect to LHV, which is the focus of the present work, in the current industrial practice it is experimentally estimated through standardized procedures (REF?? ISO), which rely on bomb calorimeters applied to small SRF samples. These procedures require time-consuming laboratory work [2], and provide untimely (typically after a few days) results affected by sampling uncertainty, which is estimated according to the applicable standard guidelines.

On the other hand, empirical models have been proposed in the literature (e.g., [5]) to predict the LHV of SRF. Although these models avoid the manual work [5], they, however, require the estimation of the SRF composition. In this respect, several studies (e.g., [6]) have recently proved that the analysis of Hyper-Spectral Images (HSIs) can be successfully fostered to identify the different composing materials, in support to solid waste recycling and treatment.

Based on these results, we developed a prototype tool to estimate the LHV of SRF. This relies on a material classification algorithm of HSIs acquired from a Short Wave Infra-Red (SWIR) camera, which feeds an ensemble of models of the literature that provide LHV estimates. The developed tool can work in real time, thus providing timely estimations of the LHV that relate to all the SRF. This avoids the sampling procedure and the related statistical uncertainty.

The paper is organized as follows. In Section 2, details on the SWIR technology are provided. In Section 3, we describe the campaign carried out to gather both the training and the test data. In Section 4, details on the Machine Learning (ML) techniques developed to classify the material are provided, together with a brief discussion of the literature models used to link the material classification to the LHV estimations. Results of the application of the methodology to SRF samples are presented in Section 5. Finally, conclusions are outlined in Section 6, which also presents the future research and deployment work for the industrial scale up of the proposed prototype solution.

2. HSI TECHNOLOGY

HSI, also referred to as chemical or spectroscopic imaging, is an emerging non-destructive technique providing accurate and detailed information about the analysed objects [7]. HSI combines the 2D spatial information retrievable from digital cameras with the 1D spectral information retrievable from spectrometers. This twofold perspective, organized in a 3D tensor called 'hypercube', allows linking the attributes of each

pixel to the chemical-physical characteristics of the material present therein [8].

2.1. SWIR Camera

Raw data were acquired with hyperspectral SWIR camera model FX17, produced by Specim Spectral Imaging. The camera is based on the push-broom technology and features a spatial resolution of 640 pixels and a spectral resolution of 224 bands. The wavelength range spans from 900 to 1700 nm. Spectral sampling is 3.5 nm/pixel and Full Width at Half Maximum is around 8 nm. Spatial and spectral distortions, known as smiley and keystones, have been compensated to a value well below a single pixel.
Light is provided by two linear halogen lights, each made up of three 20 W bulbs and a reflector with 36 degrees of aperture. To provide uniform light also on rough and non flat objects, the linear lights were installed in bright light configuration, symmetrically with respect to the optical axis. In this setting, the resulting Signal to Noise Ratio is around 1000:1 for most of the spectral range.
The materials to be scanned were placed on a 200 mm x 400 mm moving plate. Pixel size on the sample was 0,30 mm. The dimension of the hypercube obtained by scanning the plate acquiring a sequence of around 1200 frames is 640x1119x224.
The speed of the plate and the frame rate of the camera were tuned to keep the aspect ratio of the scanned objects. For each scan, we acquired:

- a white reference signal W, averaged over 100 frames on a spectralon reference target;
- a dark reference signal D, averaged over the same number of frames obtained by closing the mechanical shutter of the camera.

3. DATA COLLECTION CAMPAIGN

The data collection campaign was organized into two parts. First, we prepared the training dataset: a collection of objects of different known materials, used to build the library to train the classifier. Specifically, we gathered commonly used objects like Polyethylene Terephthalate (PET) bottles, different types of packaging (PolyproPylene (PP), Low-Density PolyEthylene (LDPE), Polystyrene (PS), cardboard, etc.), cork, High-Density PolyEthylene (HDPE) and metallic tops, different types of papers, pieces of different textiles (e.g., cotton towels, wool dresses, polyester shirts, Nylon, etc.), samples of rubbers, PolyVinyl Chloride (PVC) pipes, to cite a few. These were characterized by different morphological, geometrical and color attributes.
Then, we prepared the test data: a total number of 36 2-kg samples of SRF collected from the a2a SRF production plant in Cavaglià (Italy). For each SRF sample, a calorimeter test was performed to measure the LHV, which was compared with the values obtained from the application of the LHV estimation model to the material classifier estimations. Notice that multiple hypercubes were generated from the each SRF sample, as the area covered by the SRF sample material exceeds that of the scanner.
Figure 1 shows some known objects from the training library (left) and an example of scanned SRF (right).

(a) (b)

Fig. 1. Left: example of known object used to create the spectra training library. Right: examples of a test SRF sample.

4. ANALYTICS DEVELOPMENT

The developed analytics can be divided into three groups:

- Pre-processing, aimed at highlighting the information content of the acquired HSIs;
- Classifier, aimed at selecting the features of the HSIs that best allow distinguishing the different materials.
- LHV estimation, aimed at linking the classified materials of the SRF samples to the corresponding LHVs.

All the analytics have been developed in Python 3.7 environment, adopting standard libraries for ML (Scikit-learn, Spectral Python, Pandas, etc.) and hyperspectral data techniques ([8]).

4.1. Pre-processing

Different pre-processing are applied to hyper-spectral data. Namely, we first perform instrument calibration by applying the following equation:

$$R = \frac{I - D}{W - D}$$

where R is the calculated reflectance and I is the measured reflectance of the raw image [8].
After calibration, the Standard Normal Variate (SNV) algorithm (e.g., [9]) is used to reduce the scaling effects due to differences in signal path-length, scattering, and other effects related to the high sensitivity of the instruments to the variations of source and detector settings [8].
Background removal filter is then applied to eliminate the non informative pixels of the image. To do this, we applied a threshold value to the mean of the normalized signal, as background pixels are characterized by flat, low values spectra.
Finally, light reflections are removed by threshold filtering: the saturated spectra are characterized by flat high signals along all the wavelength.
Figure 2 shows the shapes of the pre-processed HSY (HSI) spectra of different materials, characterized by specific local minima at different wavelength. The spectra training library include ten thousand spectra from all the known objects collected.

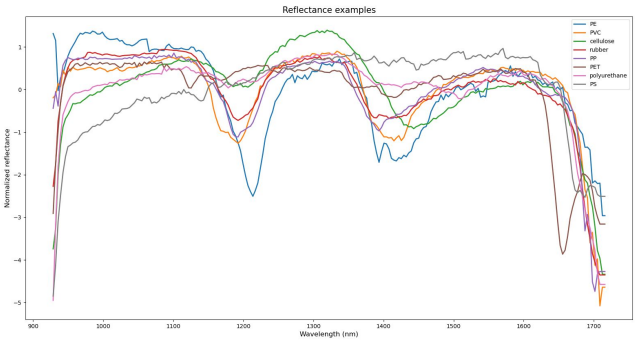

Fig. 2. Example spectra of materials.

4.2. Classifier

To build the material classifier, we first performed a feature extraction and selection procedure. Namely, we considered the first derivative of the spectra, which emphasizes the informational content of the wavelength ranges of spectra local minima. Then, we applied the Uniform Manifold Approximation and Projection (UMAP, [10]) for dimensionality reduction. This allows visualizing on a 2D space material spectra clusters (Figure 3). We can see from Figure 3 that samples characterized by similar spectra are clustered in the same region, which also correspond to materials of similar LHV values. These considerations allowed building a $n = 8$ class training library: cellulose (paper, wood, cork, fabric), rubber, PE, PET, Polyurethane, PP, PS, PVC.

Logistic Regression (LR, e.g., [9]) was selected as classifier of the labelled data of the training library, by reason of performances and simplicity. Therefore, once the classifier is obtained, it can be applied to an entire new hypercube of SRF for the classification of every image pixel.

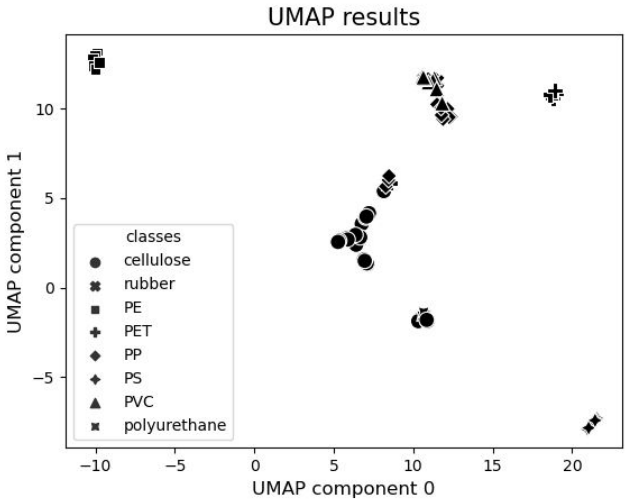

Fig. 3. UMAP results

Figure 4 shows the confusion matrix of the leave-one-group-out (LOGO) cross-validation (e.g., [9]) of the LR classifier trained on the SWIR spectra library. We set a probability threshold for classification of 0.9. That is, pixels with a class prediction probability smaller than 0.90 are assigned to a dummy class (not reported in Figure 4).
From Figure 4, we can see that all the materials in the library are well distinguished from one another, except for the class ”rubber”. This is mainly due to the complex composition of the rubbers (e.g., they often include PVC).

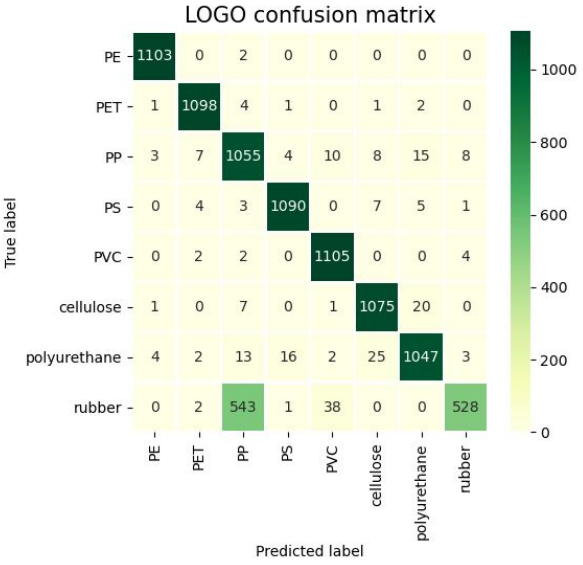

Fig. 4. Confusion matrix

	LHV min [MJ/kg]	LHV max [MJ/kg]
Rubber	25.6	46
Cellulose	17	21
PET	19	28
PP	42.6	46.2
PS	28.9	42
PVC	15	21
PE	34	46.2
Polyurethane	30	38

Table 1. LHVs for each class. LHV min is the minimum value in the literature, LHV max is the maximum.

4.3. Mapping SRF onto LHV estimations

The LHV of each SRF sample is estimated as the weighted mean of the LHVs of the different materials, the weigths being the percentage estimated by the classifier. The material LHVs have been derived from the literature ([11, 12], Table 1).
We use the following model to estimate the SRF sample LHVs:

$$LHV_{sample} = \sum_{c=1}^{n} LHV_c P_c + C_f P_{nc}$$

$$C_f = \frac{\sum_{c=1}^{n} LHV_c P_c}{\sum_{c=1}^{n} P_c}$$

where P_c is the percentage of class $c = 1, ..., n$, considering prediction probability larger than 0.9. In words, pixels with a prediction probability smaller than 0.90 are assigned a correction factor C_f.

5. RESULTS

The model trained on the SWIR spectra library is applied to the HSIs of the gathered SRF samples. This allows assigning a material class to each pixel and, thus, estimate the percentage of each material in the sample. However, in this case we do not have ground truth labels to check the performance of the classifier, although we have calorimeter measurements for the samples.
An example of SRF classification results is reported in Figure 5. There, we can see that the object borders are clearly identified on the image, which is a rough confirmation that the classification capability.
Once all the pixels are classified, the LHV values are estimated from the percentage of each class present in the HSI. The pixels composing the dummy class are usually associated with shadowed or dirty areas, thin transparent plastics, black fabrics and plastics.
Figure 6 shows the prediction of the LHV for each SRN sample. Due to the high variability of the literature LHV data (Table 1), the range bar of predicted LHV is given to visualize the uncertainty on the estimations. The maximum (minimum) LHV value corresponds to considering the maximum (minimum) LHV literature value collected for each of the eight classes. The red dots are the LHV values of the calorimeter test. An accuracy of 72% is achieved, considering the portion of the predicted LHV range containing the calorimeter LHV estimations. There are some cases where the predicted range and the target value differ significantly (i.e., sample 13, 32 and 33). These will undergo specific analysis to understand the causes, which include the influence of not tracked external factors (humidity, weather condition ...).

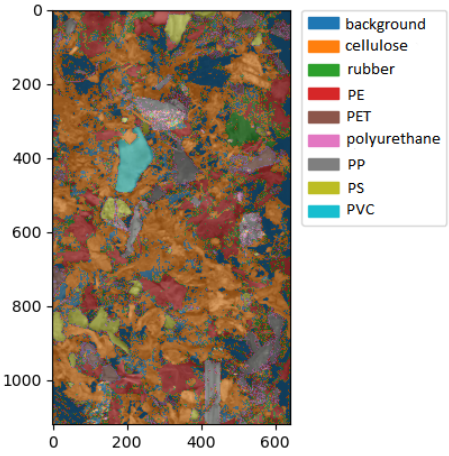

Fig. 5. Example of classification of SRF hypercubes.

6. DISCUSSION AND CONCLUSION

The aim of the present work was the development of a prototype tool for the estimation of the LHVs of the SRF, which overcomes the limitation of the gold standards techniques (i.e., calorimeter test). Specifically, we estimate the SRF material composition through a classifier applied to HSIs gathered form a SWIR camera and then map this into LHV estimations.
The results of the study are promising, although additional research work is required for the industrial scale up of the solution. Specifically, to improve the model, a wider library of ground truth material objects will be created, to enhance the classification capabilities. Yet, additional SRF calorimeter tests will performed, to reduce the uncertainty in the final LHV estimations. This uncertainty is also due to external factors, which can influence the LHV estimations. To encode them in the prediction model, an extensive campaign for SRF samples acquisition, scanning and calorimeter measuring will be carried out, which will enable the development of data-driven solutions to improve the LHV estimations.

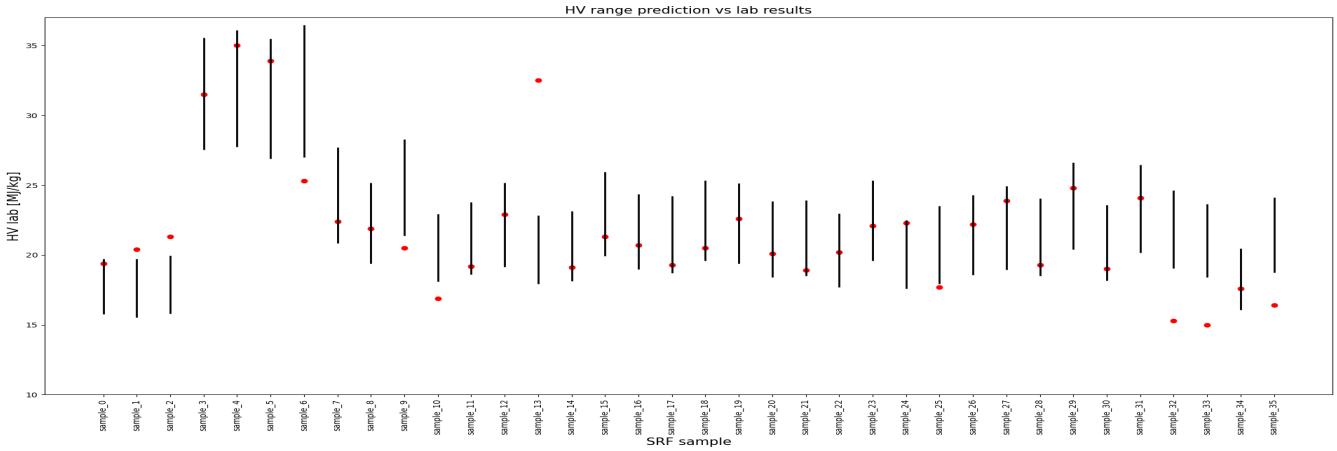

Fig. 6. HV results for each SRF sample. Black vertical lines represetn the estimated HV values, while red dots are the calorimeter HV. Some outliers are present and need a more detailed analysis to be corrected.

Moreover, the overlap among SRF pieces make the SWIR camera not able to scan all the material spectra, but those on the surface, only. To sidestep this issue, a SRF samples will be scanned multiple times, thus generating different hypercubes, each time mixing up the SRF pieces.

7. REFERENCES

[1] M.M.H. Khan, J. Havukainen, and M. Horttanainen, "Impact of utilizing solid recovered fuel on the global warming potential of cement production and waste management system: A life cycle assessment approach," *Waste Management & Research*, vol. 39, no. 4, pp. 561–572, 2021, PMID: 33357123.

[2] G.D. Agrawal, A.P.S. Rathore, and Akhilendra Gupta, "Multiple regression analysis for the estimation of energy content of municipal solid waste," *Int. J. of Environment and Waste Management*, vol. 1, pp. 376 – 390, 01 2007.

[3] S. Pieber, M. Meierhofer, A. Ragossnig, L. Brooks, R. Pomberger, and A. Curtis, "Advanced waste-splitting by sensor based sorting on the example of the mt-plant oberlaa," 11 2010.

[4] C. Birgen, E. Magnanelli, P. Carlsson, Ø. Skreiberg, J. Mosby, and M. Becidan, "Machine learning based modelling for lower heating value prediction of municipal solid waste," *Fuel*, vol. 283, pp. 118906, 2021.

[5] Y.F. Chang, C.J. Lin, J.M. Chyan, I.M. Chen, and J.E. Chang, "Multiple regression models for the lower heating value of municipal solid waste in taiwan," *Journal of Environmental Management*, vol. 85, no. 4, pp. 891–899, 2007.

[6] M. Moroni, A. Mei, A. Leonardi, E. Lupo, and F. La Marca, "Pet and pvc separation with hyperspectral imagery," *Sensors*, vol. 15, no. 1, pp. 2205–2227, 2015.

[7] S. Serranti, A. Gargiulo, and G. Bonifazi, "Characterization of post-consumer polyolefin wastes by hyperspectral imaging for quality control in recycling processes," *Waste Management*, vol. 31, no. 11, pp. 2217–2227, 2011.

[8] G. Bonifazi and S. Serranti, "Quality control by Hyper-Spectral Imaging (HSI) in solid waste recycling: logics, algorithms and procedures ," in *Image Processing: Machine Vision Applications VII*, Kurt S. Niel and Philip R. Bingham, Eds. International Society for Optics and Photonics, 2014, vol. 9024, pp. 189 – 203, SPIE.

[9] K.P. Murphy, *Probabilistic Machine Learning: An introduction*, MIT Press, 2022.

[10] Leland McInnes, John Healy, and James Melville, "Umap: Uniform manifold approximation and projection for dimension reduction," *arXiv preprint arXiv:1802.03426*, 2018.

[11] L. Costiuc, M. Tierean, S. Patachia, and L. Baltes, "Research on the heat of combustion of the plastic waste materials," *Environmental engineering and management journal*, vol. 14, 06 2015.

[12] R. Walters, S. Hackett, and R. Lyon, "Heats of combustion of high temperature polymers," *Fire and Materials - FIRE MATER*, vol. 24, pp. 245–252, 09 2000.